Published in final edited form as:

Arterioscler Thromb Vasc Biol. 2018 August ; 38(8): 1878–1889. doi:10.1161/ATVBAHA.118.311238.

Diabetic Vascular Calcification Mediated by the Collagen Receptor Discoidin Domain Receptor 1 via the Phosphoinositide 3-Kinase/Akt/Runt-Related Transcription Factor 2 Signaling Axis

Marsel Lino,
Department of Laboratory Medicine and Pathobiology, University of Toronto, Ontario, Canada

Ted Rogers Centre for Heart Research, University of Toronto, Ontario, Canada

Mark H. Wan,
Department of Laboratory Medicine and Pathobiology, University of Toronto, Ontario, Canada

Antonio S. Rocca,
Department of Laboratory Medicine and Pathobiology, University of Toronto, Ontario, Canada

Department of Medicine, University of Toronto, Ontario, Canada

David Ngai,
Department of Laboratory Medicine and Pathobiology, University of Toronto, Ontario, Canada

Ted Rogers Centre for Heart Research, University of Toronto, Ontario, Canada

Navid Shobeiri,
Department of Laboratory Medicine and Pathobiology, University of Toronto, Ontario, Canada

Ted Rogers Centre for Heart Research, University of Toronto, Ontario, Canada

Guangpei Hou,
Department of Laboratory Medicine and Pathobiology, University of Toronto, Ontario, Canada

Ted Rogers Centre for Heart Research, University of Toronto, Ontario, Canada

Chunxi Ge,
Department of Periodontics and Oral Medicine, University of Michigan School of Dentistry, Ann Arbor

Renny T. Franceschi, and
Department of Periodontics and Oral Medicine, University of Michigan School of Dentistry, Ann Arbor

Michelle P. Bendeck
Department of Laboratory Medicine and Pathobiology, University of Toronto, Ontario, Canada

Correspondence to Michelle P. Bendeck, PhD, Department of Laboratory Medicine and Pathobiology, University of Toronto, 661 University Ave, Rm 1432, Toronto, ON M5G 1M1, Canada. michelle.bendeck@utoronto.ca.

Disclosures
None.

The online-only Data Supplement is available with this article at https://www.ahajournals.org/journal/atvb/doi/suppl/10.1161/atvbaha.118.311238.

Ted Rogers Centre for Heart Research, University of Toronto, Ontario, Canada

Department of Medicine, University of Toronto, Ontario, Canada

Abstract

Objective——Vascular calcification is a common and severe complication in patients with atherosclerosis which is exacerbated by type 2 diabetes mellitus. Our laboratory recently reported that the collagen receptor discoidin domain receptor 1 (DDR1) mediates vascular calcification in atherosclerosis; however, the underlying mechanisms are unknown. During calcification, vascular smooth muscle cells transdifferentiate into osteoblast-like cells, in a process driven by the transcription factor RUNX2 (runt-related transcription factor 2). DDR1 signals via the phosphoinositide 3-kinase/Akt pathway, which is also central to insulin signaling, and upstream of RUNX2, and this led us to investigate whether DDR1 promotes vascular calcification in diabetes mellitus via this pathway.

Approach and Results——*Ddr1*$^{+/+}$*; Ldlr*$^{-/-}$ (single knock-out) and *Ddr1*$^{-/-}$*; Ldlr*$^{-/-}$ (double knock-out) mice were placed on high-fat diet for 12 weeks to induce atherosclerosis and type 2 diabetes mellitus. Von Kossa staining revealed reduced vascular calcification in the aortic arch of double knock-out compared with single knock-out mice. Immunofluorescent staining for RUNX2 was present in calcified plaques of single knock-out but not double knock-out mice. Primary vascular smooth muscle cells obtained from *Ddr1*$^{+/+}$ and *Ddr1*$^{-/-}$ mice were cultured in calcifying media. DDR1 deletion resulted in reduced calcification, a 74% reduction in p-Akt levels, and an 88% reduction in RUNX2 activity. Subcellular fractionation revealed a 77% reduction in nuclear RUNX2 levels in *Ddr1*$^{-/-}$ vascular smooth muscle cells. DDR1 associated with phosphoinositide 3-kinase, and treatment with the inhibitor wortmannin attenuated calcification. Finally, we show that DDR1 is important to maintain the microtubule cytoskeleton which is required for the nuclear localization of RUNX2.

Conclusions——These novel findings demonstrate that DDR1 promotes RUNX2 activity and atherosclerotic vascular calcification in diabetes mellitus via phosphoinositide 3-kinase/Akt signaling.

Visual Overview——An online visual overview is available for this article.

Keywords

atherosclerosis; collagen; discoidin domain receptor 1; phosphatidylinositols; vascular calcification

Vascular calcification is a severe complication in patients with cardiovascular disease and has a high prevalence in patients with type 2 diabetes (T2D) mellitus.[1–4] Characterized by the deposition of calcium phosphate crystals within the extracellular matrix, calcification contributes to the stiffening of the vasculature, resulting in severe outcomes and increased morbidity.[5] Although the relationship between vascular calcification and T2D has been previously demonstrated, our understanding of the mechanisms linking the 2 pathologies remains incomplete.[6–8] Advances in our understanding of the cellular and molecular processes contributing to the pathogenesis of vascular calcification may lead to improvements in treatment by the development of more specific therapies. In this study, we

show that discoidin domain receptor 1 (DDR1) mediates vascular calcification in an animal model of diabetic atherosclerosis, and using in vivo and in vitro experiments, we uncover potential mechanisms by which DDR1 may drive calcification.

DDR1 is a collagen-binding receptor tyrosine kinase which plays important roles regulating cellular differentiation, proliferation, migration, and matrix synthesis.[9–11] Studies using *Ldlr*-deficient mice with genetic deletion of DDR1 showed that the receptor promotes atherosclerosis and plaque instability by regulating early monocyte/macrophage infiltration and by suppressing vascular smooth muscle cell (VSMC) matrix synthesis.[12–14] Further studies demonstrated a role for DDR1 mediating vascular calcification of the atherosclerotic plaque, and in vitro studies showed that calcification of DDR1-null VSMCs was attenuated secondary to a reduction of alkaline phosphatase activity.[15] These data implicate DDR1 in the progression of vascular calcification; however, little is known about the mechanism involved.

Vascular calcification involves the transdifferentiation of VSMCs into osteochondrocyte-like cells, in a process driven by RUNX2 (runt-related transcription factor 2).[16–18] In bone development, RUNX2 is required for the commitment of mesenchymal cells to the osteochondrogenic lineage and binds to the promoters of target genes via osteoblast sensitive elements (OSEs) to regulate the transcription of genes, such as osteocalcin, alkaline phosphatase, osteopontin, and type-I collagen.[19,20] RUNX2 is phosphorylated and regulated by several intracellular kinases, including ERK1/2 (extracellular signal-related kinase 1/2),[21] P38 mitogen activated protein kinase (P38),[22] and PKB (protein kinase B/Akt).[23,24]

It is known that DDR1 binds and signals through phosphoinositide 3-kinase (PI3K), an upstream activator of Akt.[25,26] Because perturbations in PI3K/Akt signaling are a hallmark of insulin resistance and T2D,[27–29] we therefore hypothesized that DDR1 may promote vascular calcification via the PI3K/ Akt signaling pathway. Although Akt is a known stimulator of RUNX2 activity and is required for osteogenic cell differentiation in bone and VSMC,[23,24] the links between DDR1, Akt, and RUNX2 have not been previously investigated.

Materials and Methods

The data that support the findings of this study are available from the corresponding author on reasonable request.

Animals

Animal experiments were performed in accordance with the guidelines of the Canada Council on Animal Care and the approval of the University of Toronto Faculty of Medicine Animal Care Committee. *Ddr1*$^{+/+}$; *Ldlr*$^{-/-}$ (single knock-out [SKO]) and *Ddr1*$^{-/-}$; *Ldlr*$^{-/-}$ (double knock-out [DKO]) mice were generated as described previously.[12] At 6 weeks of age, male mice were fed Western-type high-fat diet (40% fat, 43% carbohydrate, 0.5% cholesterol; D05011404; Research Diets, New Brunswick, NJ) for 12 weeks to induce insulin resistance and atherosclerosis. Animals were euthanized and perfusion-fixed with 4% paraformaldehyde. Aortic arch tissue was isolated, and longitudinal sections were mounted

onto slides and stained with Von Kossa and Alizarin red to detect mineralization by the Toronto Centre for Phenogenomics. Image analysis was performed using Nikon Elements Software. Lesion size was determined by tracing between the internal elastic lamina and plaque fibrous cap and calculating the area within. Plaque calcification was determined by thresholding the areas which were positive for Von Kossa staining and calculating the percentage of Von Kossa–positive areas. Medial calcification was measured by tracing area between internal elastic lamina and the external elastic lamina and expressing the area stained positive with Alizarin red as a percentage of total medial area.

Immunohistochemistry

Paraffin-embedded aortic arch sections were stained using standard procedures. Antibodies were used at 1:100 unless otherwise indicated. Tissues were immunolabeled for RUNX2 (12556; Cell Signaling Technology, Danvers, MA), Mac-2 (galectin-3; 87985; Cell Signaling Technology), Sox-9 (sex-determining region Y-box 9; 82630; Cell Signaling Technology), BMP-2 (bone morphogenetic protein-2; ab14933; Abcam, Cambridge, United Kingdom), osteocalcin (ab93876; Abcam), 1:200 secondary goat anti-rabbit Alexa-Fluor 488 IgG antibody (A11008; Thermo Fischer Scientific, Waltham, MA), and counterstained with Hoechst-33342 (4082; Cell Signaling Technology). Staining was visualized by epifluorescence microscopy using the Nikon Eclipse Ci microscope (Nikon, Tokyo, Japan). Image analysis was performed using Nikon Elements Software. To measure nuclear RUNX2 in plaque, nuclei were detected by first thresholding for blue and then thresholding for green to measure the area within nuclei that was RUNX2 positive. To measure overall staining in plaque, a region of interest was drawn around the plaque as described above, followed by measuring stain intensity by applying a threshold on the green channel.

Cell Culture

Primary VSMCs were isolated from *Ddr1*$^{+/+}$ and *Ddr1*$^{-/-}$ C57BL/6 mouse carotid arteries as described in Hou et al.[30] Cells were propagated in DMEM (11885084; Thermo Fischer Scientific), 10% fetal bovine serum (12483020; Thermo Fischer Scientific), and 1% penicillin-streptomycin (15140122; Thermo Fischer Scientific). Experiments were performed at passages 5 to 10. For experiments relating to calcification assays and immunoblot, VSMCs were cultured for 2 or 12 days (as indicated) in normal media (DMEM with 5 mmol/L glucose [118850684; Thermo Fischer Scientific], 3% HyClone fetal bovine serum [SH3007003HI; Thermo Fischer Scientific], 1% penicillin-streptomycin [15140122]) or calcifying media (DMEM with 25 mmol/L glucose [11995065], 3% HyClone fetal bovine serum [SH3007003HI], 1% penicillin-streptomycin [15140122], 2.4 mmol/L inorganic phosphate).

Calcification Assay

VSMCs were seeded at 1563 cells/cm^2 and cultured to semiconfluency. To mimic T2D conditions and induce calcification, VSMCs were treated with calcifying media or normal media for 12 days. Calcification was determined by Alizarin red stain (2% Alizarin red stain [A5533; Sigma-Aldrich, St. Louis, MO] in water, pH 4.1) and o-cresolphthalein (C85778; Sigma-Aldrich) as previously described.[31] For Alizarin red stain, cells were fixed with 4%

paraformaldehyde for 10 minutes, stained with Alizarin red for 30 minutes, and destained with water (3×5 minutes).

Immunocytochemistry

VSMCs were grown on glass coverslips (CA48366; VWR, Radnor, PA) in 6-well plates for 2 or 12 days in normal or calcifying media. Cells were treated with dimethyl sulfoxide (control), 10 μmol/L MEK (MAPK/ERK kinase) inhibitor PD98059, or 20 μmol/L P38 inhibitor SB203580. For microtubule stabilization experiments, cells were treated with 10 μmol/L taxol (T7402; Sigma-Aldrich) for 6 hours. Cells were fixed with 4% paraformaldehyde for 10 minutes, washed 3×5 minutes in PBS, permeabilized with 0.25% Triton X-100 for 10 minutes, and blocked with 1% BSA for 1 hour. Cells were immunolabelled for RUNX2 (ab76956; Abcam) and α-tubulin (ab18251; Abcam), and secondary anti-mouse Alexa-Fluor 488 IgG (A11001; Thermo Fischer Scientific), or anti-rabbit Alexa-Fluor 488 IgG. Nuclei were stained using Hoechst-33342, and cell membrane was stained by Alexa-Fluor 647–conjugated wheat germ agglutinin (W32466; Thermo Fischer Scientific). Staining was visualized using the Nikon AR1 laser scanning confocal microscope. Images were analyzed using Image-J (National Institutes of Health, Bethesda, MD). Nuclear RUNX2 was quantified by tracing cell perimeter and nucleus. Average stain intensity was measured and expressed as nuclear:cytoplasmic ratio.

Immunoblotting

VSMCs were cultured in normal or calcifying media for 2 days and treated with 10 nmol/L insulin (12585014; Thermo Fischer Scientific), 100 nmol/L wortmannin (9951; Cell Signaling Technology), or 10 μg/mL type-I collagen (C7661; Sigma-Aldrich). For chronic lithium chloride (LiCl) treatment, VSMCs were cultured for 12 days in calcifying media with or without 20 mmol/L LiCl. Protein was isolated using 1× cell lysis buffer (9803; Cell Signaling Technology), added to 2× sample buffer (1610737; Bio-Rad Laboratories, Hercules, CA), boiled for 5 minutes, resolved by SDS-PAGE, and transferred onto PVDF (polyvinylidene fluoride; 1620177; Bio-Rad Laboratories). Antibodies were Cell Signaling Technology unless otherwise specified: ERK1/2 (9102); phospho-ERK1/2 (4376); P38 (9212); p-P38 (4631); RUNX2 (12556); DDR1 (5583); phospho-Tyr (4G10; 05–321; EMD Millipore, Billerica, MA); lamin A/C (2032); p110β (3011); p85 (4257); phospho-p85 (4228); p-Akt (9271); Akt (9272); glycogen synthase kinase (GSK) 3β (9315); p-GSK3β (phospho-GSK3β; 9336); α-SMA (α-smooth muscle actin; 14968); caspase-3 (9661); SM22-α (smooth muscle 22-α; ab212857; Abcam), Sox-9 (82630); Msx2 (Msh homeobox 2; HPA005652; Sigma-Aldrich); BMP-2 (ab14933; Abcam); GAPDH (ab9484; Abcam); β-actin (4967); horseradish peroxidase–linked rabbit secondary (7074); horseradish peroxidase–linked mouse secondary (7076). Anti–S319-P RUNX2 antibody was provided by Dr Franceschi.[22] Immunoblots were imaged using the Kodak Image Station 4000MM Pro (Kodak, Rochester, NY) and quantified using Image-J.

Subcellular Fractionation

Cells were trypsinized, pelleted by centrifugation, washed in PBS, and then resuspended in 5 mL ice-cold lysis buffer (10 mmol/L HEPES pH 7.9, 1.5 mmol/L $MgCl_2$, 10 mmol/L KCl, 0.5 mmol/L DTT (dithiothreitol), 1 complete mini EDTA-free protease inhibitor tablet

[11836170001; Roche, Basel, SUI]). Cells were lysed via Dounce homogenizer and centrifuged at 228*g* for 5 minutes. Supernatant (cytoplasmic fraction) was collected, and the pellet was resuspended in 3 mL of buffer S1 (0.25 mmol/L sucrose, 10 mmol/L $MgCl_2$, 1 protease inhibitor tablet) and overlaid by 3 mL of buffer S3 (0.88 mmol/L sucrose, 0.5 mmol/L $MgCl_2$, 1 protease inhibitor tablet). Samples were centrifuged at 2800*g* for 10 minutes at 4°C, and the pellet was isolated as the nuclear fraction.

6OSE2 Luc Plasmid Transfection and Luciferase Assay

The 6OSE2 Luc plasmid to assess Runx2 activity was amplified as previously described.[22] Briefly, 6OSE2 plasmid was transformed into competent DH5-α (Douglas Hanahan 5 alpha) *Escherichia coli* according to manufacturer's instructions (C2987H; New England Biolabs, Ipswich, MA). Plasmid DNA was extracted using plasmid Maxiprep kit (K210026; Invitrogen). VSMCs were cotransfected with 5 μg of 6OSE2 plasmid and cytomegalovirus renilla luciferase plasmid, using Lipofectamine-LTX (15338100; Thermo Fischer Scientific). Cells were cultured in normal or calcifying media for 2 days and treated with 10 μmol/L MEK inhibitor PD98059 or 20 μmol/L P38 inhibitor SB203580. Runx2 activity was assessed using Dual-Luciferase Reporter Assay according to manufacturer's instructions (E1910; Promega, Madison, WI). Luminescence was measured using the Luminat LB9507 (Berthold Technologies, Bad Wildbad, DE). Relative luminescence units were obtained by normalizing firefly luciferase signal driven by RUNX2 activity to cytomegalovirus renilla luciferase signal.

Reverse Transcription and Quantitative Real-Time Polymerase Chain Reaction

RNA was isolated using the RNeasy isolation kit according to manufacturer's protocol (74104; Qiagen, Hilden, DE). RNA was quantified using the NanoDrop 2000c (Thermo Fischer Scientific). RNA was reverse-transcribed into cDNA using the SuperScript First-Strand Synthesis Kit (11904018; Invitrogen). Quantitative real-time polymerase chain reaction was performed using SYBR advantage quantitative real-time polymerase chain reaction premix kit (Clonetech, Palo Alto, CA) using the ABI7900HT Fast Real-Time PCR System (Applied Biosystems, Foster City, CA). The following primers were used: osteocalcin (FWD 5′-GTAGTGAACAGACTCCGGC-3′, REV 5′-AGTGATACCGTAGATGCGT-3′) and Arp (FWD 5′-AGAC CTCCTTCTTCCAGGCTTT-3′, REV 5′-CCCACCTTGTCTCCA GTCTTTATC-3′). The data were analyzed using SDS 2.3 software (Applied Biosystems).

DDR1b Transfection

Plasmid containing full-length DDR1b isoform (a gift from the late Dr Wolfgang Vogel) was transformed into competent DH5-α *E coli* according to manufacturer's instructions (C2987H; New England Biolabs). Plasmid purification was performed using Maxi Prep DNA isolation kit according to manufacturer's instructions (K210026; Invitrogen). Plasmids containing DDR1b or empty vector were transfected into *Ddr1*$^{-/-}$ VSMCs using Lipofectamine-3000 according to manufacturer's instructions (L3000015; Thermo Fischer Scientific). Cells were cultured in normal media for 24 hours, followed by protein isolation and analysis by immunoblot as described above.

Immunoprecipitation of DDR1

VSMCs were seeded at 4000 cells/cm^2 on 10 cm^2 plates and cultured in normal media until semiconfluency, and then treated with calcifying medium for 2 days. Cells were treated with 10 nmol/L insulin, 100 nmol/L wortmannin, or 10 μg/mL type-I collagen (C7661; Sigma-Aldrich). Protein was isolated using radioimmunoprecipitation assay buffer (9806; Cell Signalling Technology). A total of 200 μg of protein was incubated with 1:100 DDR1 antibody overnight at 4°C. A total of 20 μL of protein-A agarose beads (9863; Cell Signaling Technology) were added to each sample and incubated for 3 hours at 4°C. Samples were centrifuged for 1 minute at 14 000*g* and then washed by resuspending in 1× cell lysis buffer and centrifuging at 14 000*g* for 1 minute. The wash step was repeated 5×. Pellets were resuspended in 50 μL of 2× sample buffer (1610737; Bio-Rad Laboratories) and prepared for immunoblot as described above.

Statistical Analyses

Data were expressed as mean±SEM. Statistical methods are summarized in the Major Resources Table in the online-only Data Supplement. Data were analyzed using GraphPad Prism Software (La Jolla, CA). Normality was assessed by D'Agostino-Pearson omnibus test followed by appropriate parametric or nonparametric analyses as indicated.

Results

DDR1 Deletion Results in Reduced Vascular Calcification and Nuclear RUNX2 Immunostaining In Vivo

Male *Ddr1*$^{+/+}$; *Ldlr*$^{-/-}$ (SKO) and *Ddr1*$^{-/-}$; *Ldlr*$^{-/-}$ (DKO) mice were fed a high-fat diabetogenic diet for 12 weeks. SKO and DKO mice gained weight and had elevated plasma glucose consistent with metabolic dysregulation observed in T2D (Figure I in the online-only Data Supplement). DKO mice had reduced body weight compared with SKO mice, which was consistent with previously reported dwarfism in this genotype[32] (Figure IA in the online-only Data Supplement). Fasting triglycerides and high-density lipoprotein cholesterol levels were not different between SKO and DKO mice while total plasma cholesterol was lower in DKO mice because of a significant reduction in low-density lipoprotein cholesterol (Figure II in the online-only Data Supplement). Tissue from the aortic arch was isolated and stained for Von Kossa to characterize atherosclerotic plaque development and calcification. Von Kossa staining revealed reduced vascular calcification in DKO mice compared with SKO littermate controls (Figure 1A and 1B). In the plaques from SKO mice, there were many cells with osteochondrocyte-like morphology (basophilic cells in lacunae), present in both mineralized tissue (Figure 1A, arrow 1) and in areas that were negative for Von Kossa staining (Figure 1A, arrow 2), which suggests that cell transdifferentiation precedes mineralization. Lesion size (Figure 1C) and the percentage of plaque area positive for calcification (Figure 1D) were significantly lower in DKO mice compared with SKO mice. The percentage area of the medial layer positive for calcification was also reduced in DKO mice albeit nonsignificantly (Figure 1E). Sections of the aortic arch from SKO and DKO mice were stained with an antibody against RUNX2, which was highly expressed in the calcifying lesions of SKO mice but not in lesions from DKO mice (Figure 1F and 1G). RUNX2 staining was present within the nuclei of plaque cells in SKO mice, as evidenced by

colocalization with nuclear Hoechst stain (Figure 1H, area circled). By contrast, nuclear RUNX2 staining was considerably reduced in aortic arch lesions from DKO mice (Figure 1I, area circled). Measurement of the area of nuclear RUNX2 staining revealed a significant reduction in DKO plaques (Figure 1J). No difference in plaque macrophage content was observed between genotypes as assessed by immunostaining for Mac-2 (Figure III in the online-only Data Supplement). Expression of osteogenic markers Sox-9, BMP-2, and osteocalcin was also measured by immunostaining aortic arch sections, revealing no significant differences in expression of these markers (Figure III in the online-only Data Supplement).

DDR1 Deletion Results in Attenuated VSMC Calcification and Is Accompanied by Reduced RUNX2 Nuclear Localization and Activity In Vitro

To study the mechanisms of calcification in vitro, primary VSMCs were isolated from *Ddr1*$^{+/+}$ and *Ddr1*$^{-/-}$ mice and cultured in normal or calcifying media for 2 or 12 days. Alizarin red stain revealed robust calcification in *Ddr1*$^{+/+}$ VSMCs after 12 days while *Ddr1*$^{-/-}$ VSMCs calcified less (Figure 2A). VSMCs cultured in normal media did not stain with Alizarin red. Calcium content in the matrix was also measured and was significantly lower in *Ddr1*$^{-/-}$ VSMCs compared with *Ddr1*$^{+/+}$ VSMCs (Figure 2B). Immunofluorescent staining for RUNX2 revealed robust nuclear localization in *Ddr1*$^{+/+}$ VSMCs and reduced levels of nuclear staining in *Ddr1*$^{-/-}$ VSMCs (Figure 2C), which was quantified by measuring a significant decrease in the ratio of nuclear to cytoplasmic stain in *Ddr1*$^{-/-}$ VSMCs (Figure 2D). RUNX2 nuclear localization was also assessed by immunoblot after nuclear fractionation of cells cultured in normal or calcifying media for 2 days (Figure 2E). Nuclear RUNX2 levels in *Ddr1*$^{-/-}$ VSMCs were 90% lower than *Ddr1*$^{+/+}$ VSMCs in normal media (Figure 2F) and 77% lower under calcifying conditions (Figure 2G). RUNX2 activity was measured after transfecting a reporter plasmid containing multiple OSEs controlling luciferase expression. RUNX2 activity was reduced by 88% in *Ddr1*$^{-/-}$ compared with *Ddr1*$^{+/+}$ VSMCs (Figure 2H). Furthermore, mRNA expression of osteocalcin (an RUNX2 target gene) was significantly reduced in *Ddr1*$^{-/-}$ VSMCs (Figure 2I). *Ddr1*$^{-/-}$ VSMCs had elevated levels of α-SMA compared with *Ddr1*$^{+/+}$ cells even under calcifying conditions, suggesting that *Ddr1*$^{-/-}$ VSMCs tend to maintain smooth muscle phenotype (Figure 2J). Because cell death by apoptosis may also contribute to calcification, we measured cleaved caspase-3 levels by immunoblotting. Cleaved caspase-3 was elevated in *Ddr1*$^{+/+}$ VSMCs after 2 days in calcifying media compared with normal media and reduced in *Ddr1*$^{-/-}$ VSMCs relative to *Ddr1*$^{+/+}$ VSMCs under both normal and calcifying conditions (Figure 2J). This suggested decreased apoptosis of *Ddr1*$^{-/-}$ VSMCs.

DDR1 Modulates p-Akt Levels in VSMCs

To test the hypothesis that DDR1 modulates RUNX2 activity via Akt signaling, Akt activation was measured by calculating the p-Akt/Akt ratio. Akt activity was reduced by 80% in *Ddr1*$^{-/-}$ compared with *Ddr1*$^{+/+}$ VSMCs under control conditions in normal media (Figure 3A and 3C). Insulin treatment resulted in a significant 2-fold increase in Akt activation in both *Ddr1*$^{+/+}$ and *Ddr1*$^{-/-}$ VSMCs. With growth in calcifying media, there was a 74% reduction in Akt phosphorylation in *Ddr1*$^{-/-}$ compared with *Ddr1*$^{+/+}$ VSMCs (Figure 3B and 3D). Insulin treatment increased p-Akt levels in *Ddr1*$^{-/-}$ but not *Ddr1*$^{+/+}$ cells, such

that significant differences between *Ddr1*$^{-/-}$ and *Ddr1*$^{+/+}$ cells were abolished (Figure 3D). These findings suggest that Akt signaling is perturbed with growth of VSMCs in calcifying media and that loss of DDR1 lowers p-Akt expression. When a plasmid encoding full-length *Ddr1b* was used to reconstitute expression in *Ddr1*$^{-/-}$ VSMCs, Akt phosphorylation was increased (Figure 3E), suggesting a direct effect of DDR1 expression on p-Akt levels.

DDR1 Mediates VSMC Calcification Through the PI3K/Akt Signaling Axis

To assess the effect of the PI3K/Akt signaling axis on vascular calcification in vitro, *Ddr1*$^{+/+}$ or *Ddr1*$^{-/-}$ VSMCs were cultured in calcifying media for 12 days and treated daily with insulin (10 nmol/L) to stimulate PI3K, or wortmannin (100 nmol/L) to inhibit PI3K, then stained with Alizarin red to assess calcification. Insulin augmented, whereas wortmannin attenuated calcification in both cell types, albeit with much higher levels of calcification present in *Ddr1*$^{+/+}$ compared with *Ddr1*$^{-/-}$ VSMCs (Figure 4A). Next, we performed immunoprecipitation experiments to test the association between DDR1 and PI3K after treatment with type-1 collagen. Type-1 collagen treatment induced tyrosine phosphorylation of DDR1 (pY) and increased the association of DDR1 with the active PI3K subunits phospho-p85 and p110β (Figure 4B). Treatment with insulin also increased the association of DDR1 and PI3K and potentiated the effect of type-I collagen when both were added together (Figure 4B). This suggests cross talk between DDR1 and insulin signaling pathways. By contrast, treatment with wortmannin reduced the association of PI3K and DDR1 (Figure 4B).

DDR1 Deletion Affects ERK1/2 and P38 Activity; P38 Is Required for RUNX2 Activation

Previous studies have shown that RUNX2 activity is dependent on phosphorylation by ERK1/2 and P38, therefore we measured these kinases in VSMCs cultured in calcifying media. Phospho-ERK1/2 (Figure 5A) and phospho-P38 (Figure 5B) levels were reduced in *Ddr1*$^{-/-}$ VSMCs compared with *Ddr1*$^{+/+}$ cells. However, inhibition of these kinases (with MEKi for ERK1/2 or P38i) did not alter the nuclear localization of RUNX2 compared with dimethyl sulfoxide controls (Figure 5C). By contrast, P38 inhibition markedly decreased RUNX2 activity measured by luciferase assay in both cell types while ERK1/2 inhibition had no significant effect (Figure 5D). Probing a Western blot for phospho-RUNX2, we showed that P38 inhibition almost completely abolished RUNX2 phosphorylation in *Ddr1*$^{+/+}$ cells (Figure 5E). Taken together, these data suggest that although DDR1 is important for the activation of both ERK1/2 and P38, P38 but not ERK1/2 activity is required to phosphorylate and activate RUNX2 in VSMCs.

GSK3β Inhibition Results in an Increase in Osteochondrogenic Marker Expression in *Ddr1*$^{+/+}$ but Not *Ddr1*$^{-/-}$ VSMCs

GSK3β is a kinase downstream of Akt which phosphorylates RUNX2 at S369, S373, and S377, suppressing its transcriptional activity.[33] Akt is known to phosphorylate and inhibits GSK3β, and furthermore the loss of GSK3β is known to promote osteogenesis. We sought to determine whether GSK3β is implicated in DDR1-mediated vascular calcification. We found that phospho-GSK3β levels were decreased in *Ddr1*$^{-/-}$ VSMCs (Figure 6A), which would indicate increased GSK3β activity which could in turn lead to the suppression of RUNX2 activity and VSMC calcification. To modulate GSK3β pharmacologically, VSMCs

were cultured in calcifying media, treated daily with the GSK3β inhibitor LiCl(20 mmol/L) for 12 days, and probed for expression of smooth muscle and osteochondrogenic markers (Figure 6B). *Ddr1*$^{-/-}$ VSMCs had significantly elevated expression of smooth muscle markers α-SMA and SM22α compared with *Ddr1*$^{+/+}$ VSMCs under control conditions (Figure 6C and 6D). Levels of the osteochondrogenic markers (Sox-9, Msx2, RUNX2, and BMP-2) were low and not significantly different between *Ddr1*$^{+/+}$ and *Ddr1*$^{-/-}$ VSMCs under control condition (Figure 6E–6H). GSK3β inhibition with LiCl resulted in a significant increase in levels of osteochondrogenic markers RUNX2, Sox-9, and BMP-2 in *Ddr1*$^{+/+}$ VSMCs (Figure 6E–GH). These findings demonstrate an inhibitory role of GSK3β on VSMC transdifferentiation to the osteochondrogenic phenotype. Taken together, these data indicate that DDR1's role in promoting VSMC calcification is at least in part mediated by GSK3β.

Microtubules Are Disrupted in *Ddr1*$^{-/-}$ VSMCs and Stabilization With Taxol Rescues RUNX2 Nuclear Localization but Not Activity

In addition to the phospho-signaling cascades that alter RUNX2 activation, the microtubule cytoskeleton regulates RUNX2 localization and activity[34]; however, this has not been studied in VSMCs nor has the cytoskeleton been investigated in *Ddr1*$^{-/-}$ VSMCs. Immunostaining for α-tubulin revealed alterations in cell morphology and microtubule organization in *Ddr1*$^{-/-}$ VSMCs grown in normal or calcifying media. *Ddr1*$^{-/-}$ VSMCs were larger, and tubulin staining was more diffuse in the cytoplasm with less prominent microtubules than in *Ddr1*$^{+/+}$ VSMCs (Figure 7A). Staining for RUNX2 was localized in the nucleus of *Ddr1*$^{+/+}$ VSMCs and mostly cytoplasmic in *Ddr1*$^{-/-}$ VSMCs (Figure 7B). Cells were treated with taxol to stabilize microtubules, which enhanced tubulin staining and resulted in the appearance of short microtubules in *Ddr1*$^{-/-}$ VSMCs (Figure IV in the online-only Data Supplement). Taxol treatment resulted in a significant increase in RUNX2 nuclear staining in *Ddr1*$^{-/-}$ VSMCs (Figure 7B and 7C). However, RUNX2-driven luciferase activity was inhibited by taxol in both *Ddr1*$^{+/+}$ and *Ddr1*$^{-/-}$ VSMCs (Figure 7D). The latter is possibly because taxol treatment leads to the inhibitory phosphorylation of RUNX2 on S125, precluding the assessment of RUNX2 activity under these conditions.[35]

Discussion

Atherosclerotic vascular calcification is exacerbated by T2D, but our understanding of the mechanisms involved is incomplete. Here, we report for the first time that DDR1 signals via the PI3K/Akt pathway to modulate RUNX2 activity, promoting VSMC calcification in vivo and in vitro. Using *Ldlr*$^{-/-}$ mice fed a high-fat diabetogenic diet, we detected significant vascular calcification and robust nuclear RUNX2 localization in calcific atherosclerotic lesions of DDR1-positive, but not DDR1-deficient mice. The reduction in vascular calcification was consistent with our previously published findings in mice fed an atherogenic diet[15] and adds evidence that DDR1 influences calcification in a mouse model of diabetes mellitus. Furthermore, our in vitro experiments demonstrate a mechanistic pathway, whereby DDR1 influences RUNX2-dependant VSMC transdifferentiation via PI3K/Akt and GSK3β signaling.

We have observed some differences comparing *Ldlr*$^{-/-}$ mice fed a diabetogenic diet versus our previous studies with mice fed an atherogenic diet. First, plasma cholesterol was significantly reduced in DDR1-deficient mice fed the diabetogenic diet whereas this was not the case in our previous studies of mice fed an atherogenic diet.[15] Second, there was no difference in macrophage accumulation in plaques of DDR1-deficient mice fed the diabetogenic diet whereas our previous studies showed decreased macrophage accumulation in DDR1-deficient mice fed an atherogenic diet.[13] The reasons for these differences are likely because of differences in the 2 diets and will require further investigation. However, consistent across both models was a dramatic decrease in vascular calcification in DDR1-deficient mice which occurred irrespective of changes in circulating lipids and local inflammation. Moreover, we observed significant reductions in the ability of DDR1-deficient VSMCs in culture to transdifferentiate to osteochondrocytic cells, with experiments pointing to a reduction in activity of the critical transcriptional mediator RUNX2. Because this data strongly suggest VSMC-specific functions for DDR1, we turned our attention to in vitro experiments with these cells for further investigation of the mechanisms involved.

It has been shown that DDR1 binds to PI3K,[25] a kinase known to regulate proliferation, cell fate decisions, and insulin signaling.[36,37] PI3K signaling through Akt regulates osteogenesis,[24] and it has been shown previously to drive VSMC calcification by inducing RUNX2 activity.[23] Given the central role of the PI3K/Akt pathway in both insulin signaling and osteogenesis, we focused our attention on this pathway. We show that in VSMCs activation of DDR1 with type-I collagen resulted in the association of the receptor with the PI3K subunits p110β and p85. This interaction was attenuated after treatment with the PI3K inhibitor wortmannin, which also inhibited VSMC calcification. DDR1 deficiency resulted in reduced phosphorylation of the downstream kinase Akt that was rescued by reconstitution of DDR1 expression in DDR1-deficient VSMCs. The association of DDR1 with PI3K and phosphorylation of Akt were also observed after insulin stimulation of VSMCs, suggesting there may be cross talk between DDR1 and insulin receptor signaling. These findings support the hypothesis that DDR1 promotes RUNX2 activity and vascular calcification via PI3K/Akt signaling.

ERK1/2 and P38 have also been shown to regulate RUNX2 activity during osteogenesis.[21,22] In osteoblasts, ERK1/2 phosphorylates RUNX2 at S301 and S319, inducing RUNX2 transcriptional activity.[21] P38 also phosphorylates RUNX2 at S319, and inhibition of P38 results in reduced RUNX2 activity,[22] while P38 mutation results in reduced bone mass.[38] Less is known about these pathways in VSMC calcification. We found that although both ERK1/2 and P38 phosphorylation were reduced in *Ddr1*$^{-/-}$ VSMCs, inhibition of these kinases did not affect RUNX2 nuclear localization in VSMCs. However, P38 inhibition abolished RUNX2 activity in both *Ddr1*$^{+/+}$ and *Ddr1*$^{-/-}$ VSMCs and reduced the phosphorylation of RUNX2 at S319, suggesting that P38 is required for RUNX2 phosphorylation and activity. By contrast, ERK1/2 inhibition did not significantly affect activity in either cell type. These findings suggest that nuclear localization and phosphorylation of RUNX2 are both required for transcriptional activity of RUNX2 to occur and that these 2 processes are regulated by different mechanisms downstream of DDR1.

The mechanisms by which Akt regulates RUNX2 are complex; for example, in tumor cells, RUNX2 activity stability and nuclear translocation are all affected by Akt through direct and indirect mechanisms.[39] Akt directly phosphorylates and activates RUNX2, but in addition, Akt suppresses GSK3β, a known inhibitor of RUNX2. In our studies, we show a role for Akt suppression of GSK3β activity in regulating vascular calcification. We propose that DDR1-positive VSMCs robust Akt activity results in the inhibitory phosphorylation of GSK3β, which relieves suppression of RUNX2, allowing transdifferentiation and calcification. Conversely, *Ddr1*$^{-/-}$ VSMCs had increased GSK3β activity as determined by reduced expression of p-GSK3β, which resulted in the suppression of RUNX2 and calcification. GSK3β inhibition with LiCl resulted in the upregulation of multiple osteogenic markers with a concomitant reduction in smooth muscle markers in *Ddr1*$^{+/+}$ VSMCs, demonstrating that inhibition of GSK3β is proosteogenic. However, LiCl did not affect the expression of osteogenic markers in *Ddr1*$^{-/-}$ VSMCs, suggesting that suppression of GSK3β is insufficient for RUNX2 activation and calcification in these cells. It is likely that p38K mediated phosphorylation of RUNX2 and other as yet unknown mechanisms are required.

In addition to activation of RUNX2 through kinase signaling, previous studies have demonstrated interactions between RUNX2 and the microtubule and actin cytoskeletons which can influence osteoblastic differentiation or tumor cell metastasis.[34,35,40,41] Staining for α-tubulin revealed that the microtubules were disorganized in *Ddr1*$^{-/-}$ VSMCs, leading us to investigate whether microtubules might play a role in RUNX2 activation in VSMCs. We found that treatment of *Ddr1*$^{-/-}$ VSMCs with taxol to stabilize microtubules rescued RUNX2 nuclear localization. However, the fact that taxol inhibits RUNX2 precludes the full analysis of activity.[35] Moreover, our findings stand in contrast to studies previously performed in tumor cells, where microtubule stabilization resulted in sequestration of RUNX2 in the cytoplasm,[34] thus preventing transcriptional activity. This suggests a different mechanism for RUNX2 regulation by microtubules in VSMCs. Finally, it is important to note that GSK3β is a potent suppressor of microtubule assembly and stability (reviewed by Zhou and Snider[42]). Therefore, the elevated GSK3β activity in DDR1-deficient cells might lead to microtubule destabilization preventing RUNX2 nuclear localization, as well as to the direct inhibitory phosphorylation of RUNX2 at S369, 373, or 377. Further investigation into the regulation of RUNX2 by DDR1-mediated signaling and regulation of cytoskeletal organization will improve our understanding of the molecular mechanisms underlying the pathogenesis of vascular calcification.

Conclusions

The present study is the first to report that DDR1 promotes vascular calcification in T2D via PI3K/Akt-mediated signaling to induce RUNX2 activity. The regulation of GSK3β activity and microtubule assembly are important downstream mechanisms involved in VSMC calcification.

Supplementary Material

Refer to Web version on PubMed Central for supplementary material.

Acknowledgments

We thank Laura-lee Caruso for animal husbandry, Sean Cai who helped with optimization of immunostaining, and Emily Luk who helped amplify and optimize the 6OSE2 Luc plasmid transfection.

Sources of Funding

Canadian Institutes for Health Research grant MOP133592 to M.P. Bendeck. M. Lino was supported by scholarships from the Heart & Stroke Richard Lewar Centre of Excellence and the Banting and Best Diabetes Centre. D. Ngai and N. Shobeiri were also supported by scholarships from the Banting and Best Diabetes Center. M.P. Bendeck was a Career Investigator of the Heart and Stroke Foundation of Ontario.

Nonstandard Abbreviations and Acronyms

DDR1	discoidin domain receptor 1
DKO	double knock-out
ERK1/2	extracellular signal-related kinase 1/2
GSK3β	glycogen synthase kinase 3β
LiCl	lithium chloride
OSE	osteoblast sensitive elements
P38	P38 mitogen activated protein kinase
PI3K	phosphoinositide 3-kinase
RUNX2	runt-related transcription factor 2
SKO	single knock-out
T2D	type 2 diabetes
VSMC	vascular smooth muscle cell

References

1. Sage AP, Tintut Y, Demer LL. Regulatory mechanisms in vascular calcification. Nat Rev Cardiol. 2010;7:528–536. doi: 10.1038/nrcardio.2010.115. [PubMed: 20664518]
2. Stabley JN, Towler DA. Arterial calcification in diabetes mellitus: preclinical models and translational implications. Arterioscler Thromb Vasc Biol. 2017;37:205–217. doi: 10.1161/ATVBAHA.116.306258. [PubMed: 28062508]
3. Yahagi K, Kolodgie FD, Lutter C, Mori H, Romero ME, Finn AV, Virmani R. Pathology of human coronary and carotid artery atherosclerosis and vascular calcification in diabetes mellitus. Arterioscler Thromb Vasc Biol. 2017;37:191–204. doi: 10.1161/ATVBAHA.116.306256. [PubMed: 27908890]
4. Benjamin EJ, Blaha MJ, Chiuve SE, et al.; American Heart Association Statistics Committee and Stroke Statistics Subcommittee. Heart disease and stroke statistics-2017 update: a report from the American Heart Association. Circulation. 2017;135:e146–e603. doi: 10.1161/CIR.0000000000000485. [PubMed: 28122885]
5. Abedin M, Tintut Y, Demer LL. Vascular calcification: mechanisms and clinical ramifications. Arterioscler Thromb Vasc Biol. 2004;24:1161–1170. doi: 10.1161/01.ATV.0000133194.94939.42. [PubMed: 15155384]

6. Snell-Bergeon JK, Budoff MJ, Hokanson JE. Vascular calcification in diabetes: mechanisms and implications. Curr Diab Rep. 2013;13:391–402. doi: 10.1007/s11892-013-0379-7. [PubMed: 23526400]
7. Nguyen N, Naik V, Speer MY. Diabetes mellitus accelerates cartilaginous metaplasia and calcification in atherosclerotic vessels of LDLr mutant mice. Cardiovasc Pathol. 2013;22:167–175. doi: 10.1016/j.carpath.2012.06.007. [PubMed: 22818582]
8. Rogers MA, Aikawa E. Modifying vascular calcification in diabetes mellitus: contribution of O-GlcNAcylation. Circ Res. 2014;114:1074–1076. doi: 10.1161/CIRCRESAHA.114.303684. [PubMed: 24677232]
9. Curat CA, Eck M, Dervillez X, Vogel WF. Mapping of epitopes in dis-coidin domain receptor 1 critical for collagen binding. J Biol Chem. 2001;276:45952–45958. doi: 10.1074/jbc.M104360200. [PubMed: 11598108]
10. Leitinger B Discoidin domain receptor functions in physiological and pathological conditions. Int Rev Cell Mol Biol. 2014;310:39–87. doi: 10.1016/B978-0-12-800180-6.00002-5. [PubMed: 24725424]
11. Vogel W, Gish GD, Alves F, Pawson T. The discoidin domain receptor tyrosine kinases are activated by collagen. Mol Cell. 1997;1:13–23. [PubMed: 9659899]
12. Franco C, Hou G, Ahmad PJ, Fu EY, Koh L, Vogel WF, Bendeck MP. Discoidin domain receptor 1 (ddr1) deletion decreases atherosclerosis by accelerating matrix accumulation and reducing inflammation in low-density lipoprotein receptor-deficient mice. Circ Res. 2008;102:1202–1211. doi: 10.1161/CIRCRESAHA.107.170662. [PubMed: 18451340]
13. Franco C, Ahmad PJ, Hou G, Wong E, Bendeck MP. Increased cell and matrix accumulation during atherogenesis in mice with vessel wall-specific deletion of discoidin domain receptor 1. Circ Res. 2010;106:1775–1783. doi: 10.1161/CIRCRESAHA.109.213637. [PubMed: 20448217]
14. Franco C, Britto K, Wong E, Hou G, Zhu SN, Chen M, Cybulsky MI, Bendeck MP. Discoidin domain receptor 1 on bone marrow-derived cells promotes macrophage accumulation during atherogenesis. Circ Res. 2009;105:1141–1148. doi: 10.1161/CIRCRESAHA.109.207357. [PubMed: 19834008]
15. Ahmad PJ, Trcka D, Xue S, Franco C, Speer MY, Giachelli CM, Bendeck MP. Discoidin domain receptor-1 deficiency attenuates atherosclerotic calcification and smooth muscle cell-mediated mineralization. Am J Pathol. 2009;175:2686–2696. doi: 10.2353/ajpath.2009.080734. [PubMed: 19893047]
16. Lin ME, Chen T, Leaf EM, Speer MY, Giachelli CM. Runx2 expression in smooth muscle cells is required for arterial medial calcification in mice. Am J Pathol. 2015;185:1958–1969. doi: 10.1016/j.ajpath.2015.03.020. [PubMed: 25987250]
17. Speer MY, Yang HY, Brabb T, Leaf E, Look A, Lin WL, Frutkin A, Dichek D, Giachelli CM. Smooth muscle cells give rise to osteochondrogenic precursors and chondrocytes in calcifying arteries. Circ Res. 2009;104:733–741. doi: 10.1161/CIRCRESAHA.108.183053. [PubMed: 19197075]
18. Sun Y, Byon CH, Yuan K, Chen J, Mao X, Heath JM, Javed A, Zhang K, Anderson PG, Chen Y. Smooth muscle cell-specific runx2 deficiency inhibits vascular calcification. Circ Res. 2012;111:543–552. doi: 10.1161/CIRCRESAHA.112.267237. [PubMed: 22773442]
19. Choi JY, Pratap J, Javed A, Zaidi SK, Xing L, Balint E, Dalamangas S, Boyce B, van Wijnen AJ, Lian JB, Stein JL, Jones SN, Stein GS. Subnuclear targeting of Runx/Cbfa/AML factors is essential for tissue-specific differentiation during embryonic development. Proc Natl Acad Sci USA. 2001;98:8650–8655. doi: 10.1073/pnas.151236498. [PubMed: 11438701]
20. Stein GS, Lian JB, van Wijnen AJ, Stein JL, Montecino M, Javed A, Zaidi SK, Young DW, Choi JY, Pockwinse SM. Runx2 control of organization, assembly and activity of the regulatory machinery for skeletal gene expression. Oncogene. 2004;23:4315–4329. doi: 10.1038/sj.onc.1207676. [PubMed: 15156188]
21. Ge C, Xiao G, Jiang D, Yang Q, Hatch NE, Roca H, Franceschi RT. Identification and functional characterization of ERK/MAPK phosphorylation sites in the Runx2 transcription factor. J Biol Chem. 2009;284:32533–32543. doi: 10.1074/jbc.M109.040980. [PubMed: 19801668]

22. Ge C, Yang Q, Zhao G, Yu H, Kirkwood KL, Franceschi RT. Interactions between extracellular signal-regulated kinase ½ and p38 MAP kinase pathways in the control of RUNX2 phosphorylation and transcriptional activity. J Bone Miner Res. 2012;27:538–551. doi: 10.1002/jbmr.561. [PubMed: 22072425]
23. Byon CH, Javed A, Dai Q, Kappes JC, Clemens TL, Darley-Usmar VM, McDonald JM, Chen Y. Oxidative stress induces vascular calcification through modulation of the osteogenic transcription factor Runx2 by AKT signaling. J Biol Chem. 2008;283:15319–15327. doi: 10.1074/jbc.M800021200. [PubMed: 18378684]
24. Fujita T, Azuma Y, Fukuyama R, Hattori Y, Yoshida C, Koida M, Ogita K, Komori T. Runx2 induces osteoblast and chondrocyte differentiation and enhances their migration by coupling with PI3K-Akt signaling. J Cell Biol. 2004;166:85–95. doi: 10.1083/jcb.200401138. [PubMed: 15226309]
25. Lemeer S, Bluwstein A, Wu Z, Leberfinger J, Müller K, Kramer K, Kuster B. Phosphotyrosine mediated protein interactions of the discoidin domain receptor 1. J Proteomics. 2012;75:3465–3477. doi: 10.1016/j.jprot.2011.10.007. [PubMed: 22057045]
26. Dejmek J, Dib K, Jönsson M, Andersson T. Wnt-5a and G-protein signaling are required for collagen-induced DDR1 receptor activation and normal mammary cell adhesion. Int J Cancer. 2003;103:344–351. doi: 10.1002/ijc.10752. [PubMed: 12471617]
27. Nigro J, Osman N, Dart AM, Little PJ. Insulin resistance and atherosclerosis. Endocr Rev. 2006;27:242–259. doi: 10.1210/er.2005-0007. [PubMed: 16492903]
28. Muoio DM, Newgard CB. Mechanisms of disease: molecular and metabolic mechanisms of insulin resistance and beta-cell failure in type 2 diabetes. Nat Rev Mol Cell Biol. 2008;9:193–205. doi: 10.1038/nrm2327. [PubMed: 18200017]
29. Prudente S, Morini E, Trischitta V. Insulin signaling regulating genes: effect on T2DM and cardiovascular risk. Nat Rev Endocrinol. 2009;5:682–693. doi: 10.1038/nrendo.2009.215. [PubMed: 19924153]
30. Hou G, Vogel W, Bendeck MP. The discoidin domain receptor tyrosine kinase DDR1 in arterial wound repair. J Clin Invest. 2001;107:727–735. doi: 10.1172/JCI10720. [PubMed: 11254672]
31. Jono S, Nishizawa Y, Shioi A, Morii H. Parathyroid hormone-related peptide as a local regulator of vascular calcification. Its inhibitory action on *in vitro* calcification by bovine vascular smooth muscle cells. Arterioscler Thromb Vasc Biol. 1997;17:1135–1142. [PubMed: 9194765]
32. Vogel WF, Aszódi A, Alves F, Pawson T. Discoidin domain receptor 1 tyrosine kinase has an essential role in mammary gland development. Mol Cell Biol. 2001;21:2906–2917. doi: 10.1128/MCB.21.8.2906-2917.2001. [PubMed: 11283268]
33. Kugimiya F, Kawaguchi H, Ohba S, Kawamura N, Hirata M, Chikuda H, Azuma Y, Woodgett JR, Nakamura K, Chung UI. GSK-3beta controls osteogenesis through regulating Runx2 activity. PLoS One. 2007;2:e837. doi: 10.1371/journal.pone.0000837. [PubMed: 17786208]
34. Pockwinse SM, Rajgopal A, Young DW, Mujeeb KA, Nickerson J, Javed A, Redick S, Lian JB, van Wijnen AJ, Stein JL, Stein GS, Doxsey SJ. Microtubule-dependent nuclear-cytoplasmic shuttling of Runx2. J Cell Physiol. 2006;206:354–362. doi: 10.1002/jcp.20469. [PubMed: 16110492]
35. Zou W, Greenblatt MB, Brady N, Lotinun S, Zhai B, de Rivera H, Singh A, Sun J, Gygi SP, Baron R, Glimcher LH, Jones DC. The microtubule-associated protein DCAMKL1 regulates osteoblast function via repression of Runx2. J Exp Med. 2013;210:1793–1806. doi: 10.1084/jem.20111790. [PubMed: 23918955]
36. Vanhaesebroeck B, Guillermet-Guibert J, Graupera M, Bilanges B. The emerging mechanisms of isoform-specific PI3K signalling. Nat Rev Mol Cell Biol. 2010;11:329–341. doi: 10.1038/nrm2882. [PubMed: 20379207]
37. Vanhaesebroeck B, Stephens L, Hawkins P. PI3K signalling: the path to discovery and understanding. Nat Rev Mol Cell Biol. 2012;13:195–203. doi: 10.1038/nrm3290. [PubMed: 22358332]
38. Greenblatt MB, Shim JH, Zou W, et al. The p38 MAPK pathway is essential for skeletogenesis and bone homeostasis in mice. J Clin Invest. 2010;120:2457–2473. doi: 10.1172/JCI42285. [PubMed: 20551513]

39. Cohen-Solal KA, Boregowda RK, Lasfar A. RUNX2 and the PI3K/AKT axis reciprocal activation as a driving force for tumor progression. Mol Cancer. 2015;14:137. doi: 10.1186/s12943-015-0404-3. [PubMed: 26204939]

40. Tandon M, Othman AH, Ashok V, Stein GS, Pratap J. The role of Runx2 in facilitating autophagy in metastatic breast cancer cells. J Cell Physiol. 2018;233:559–571. doi: 10.1002/jcp.25916. [PubMed: 28345763]

41. Zouani OF, Rami L, Lei Y, Durrieu MC. Insights into the osteoblast precursor differentiation towards mature osteoblasts induced by continuous BMP-2 signaling. Biol Open. 2013;2:872–881. doi: 10.1242/bio.20134986. [PubMed: 24143273]

42. Zhou FQ, Snider WD. GSK-3b and microtubule assembly in axons. Science. 2005;308:211–214 [PubMed: 15825222]

Highlights

- Discoidin domain receptor 1 (DDR1) deletion resulted in attenuated vascular calcification and reduced RUNX2 (runt-related transcription factor 2) levels in atherosclerotic lesions in an animal model of type 2 diabetes mellitus.
- Loss of DDR1 led to reduced calcification, reduced p-Akt levels, and attenuated RUNX2 activity and nuclear localization in vascular smooth muscle cells cultured under calcifying conditions in vitro.
- Phosphoinositide 3-kinase associated with active DDR1, and restoration of DDR1 expression in DDR1-null vascular smooth muscle cells rescued Akt activation.
- DDR1-deficient vascular smooth muscle cells exhibited enhanced glycogen synthase kinase 3β activation and impaired microtubule organization, possible reasons for the attenuated activity and nuclear localization of RUNX2.

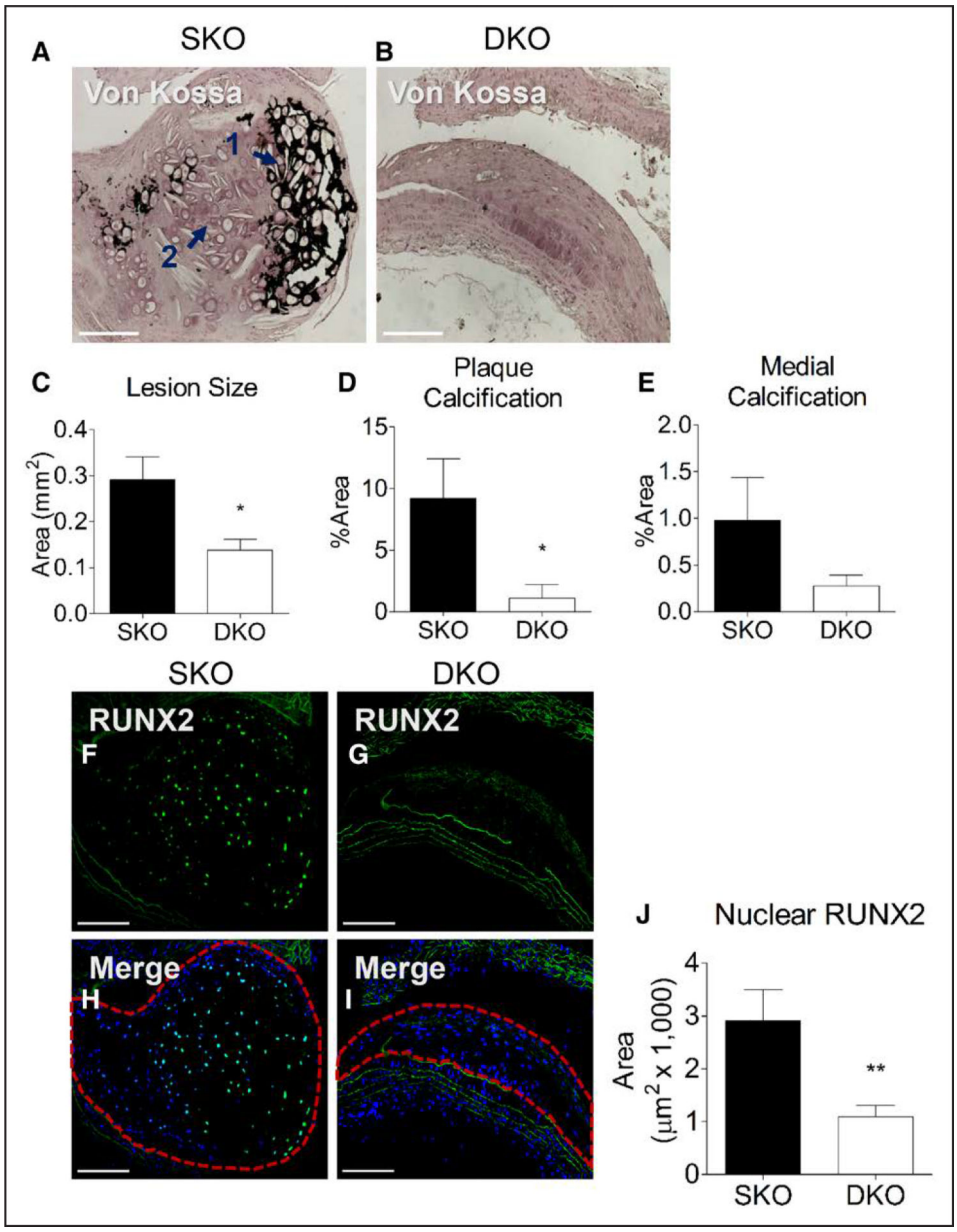

Figure 1.

Discoidin domain receptor 1 (DDR1) deletion results in reduced vascular calcification and nuclear RUNX2 (runt-related transcription factor 2) immunostaining. Aortic arches from *Ddr1*$^{+/+}$*; Ldlr*$^{-/-}$ (single knock-out [SKO]; n=12) and *Ddr1*$^{-/-}$*; Ldlr*$^{-/-}$ (double knock-out [DKO]; n=10) mice fed high-fat diet for 12 wk were stained with Von Kossa (**A** and **B**). Lesion size (**C**) and plaque (**D**) and medial (**E**) calcification were quantified. RUNX2 staining (**F** and **G**) was evident in calcifying plaques from SKO mice (**H**, circled area) and reduced in DKO plaques **(I**, circled area). Nuclear RUNX2 expression was reduced in DKO plaque (**J**). Scale bars, 200 μm. Statistical analysis was performed by Student *t* test (**C**, **E**, and **J**) and Mann-Whitney test (**D**) **P*<0.05, ***P*<0.01.

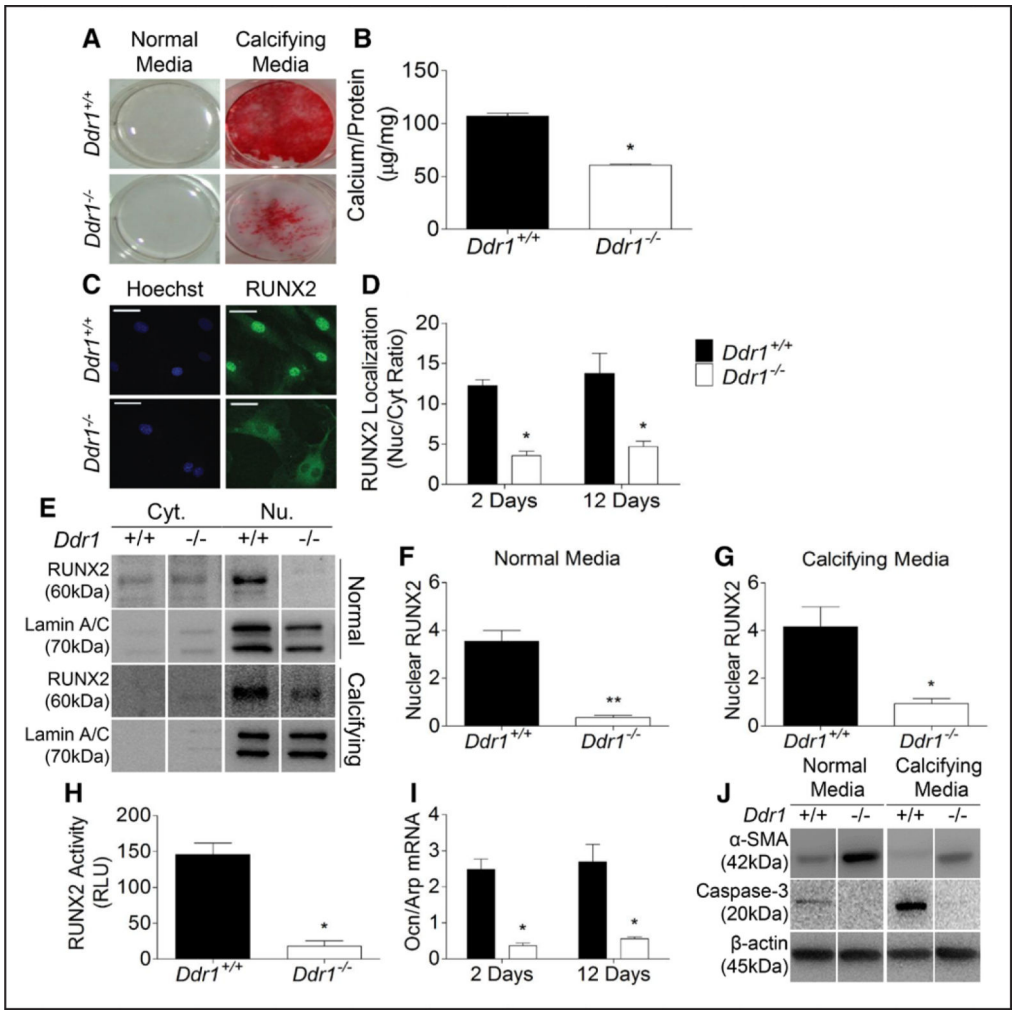

Figure 2.

Discoidin domain receptor 1 (DDR1) deletion results in attenuated vascular smooth muscle cell (VSMC) calcification and is accompanied by reduced RUNX2 (runt-related transcription factor 2) nuclear localization and activity in vitro. *Ddr1*$^{+/+}$ and *Ddr1*$^{-/-}$ VSMCs were cultured in normal or calcifying media for 2 or 12 d. Alizarin red stain (**A**) and o-cresolphthalein assay (**B**) showed reduced calcification in *Ddr1*$^{-/-}$ VSMCs after 12 d in calcifying media. RUNX2 immunostaining revealed reduced nuclear localization of RUNX2 in *Ddr1*$^{-/-}$ VSMCs (**C**), which was significant after 2 or 12 d in calcifying media (**D**). Subcellular fractionation of VSMCs showed reduced nuclear RUNX2 levels in *Ddr1*$^{-/-}$ VSMCs (**E**) cultured in normal (**F**) and calcifying (**G**) conditions for 2 d. RUNX2 transcriptional activity was reduced in *Ddr1*$^{-/-}$ VSMCs after 2 d in calcifying media (**H**). Osteocalcin mRNA was reduced at 2 and 12 d in calcifying media (**I**). α-SMA (smooth muscle α-actin) was increased while cleaved caspase-3 was reduced in *Ddr1*$^{-/-}$ compared with *Ddr1*$^{+/+}$ VSMCs after 2-d culture in normal or calcifying media (**J**). **B** and **F**–**H**, Student *t* test (**P*<0.05, ***P*<0.01). **D** and **I**, Two-way ANOVA with Bonferroni post hoc test (**P*<0.05 comparing *Ddr1*$^{+/+}$ to *Ddr1*$^{-/-}$ VSMCs). **C**, Scale bars, 20 μm. RLU indicates relative luminescence units.

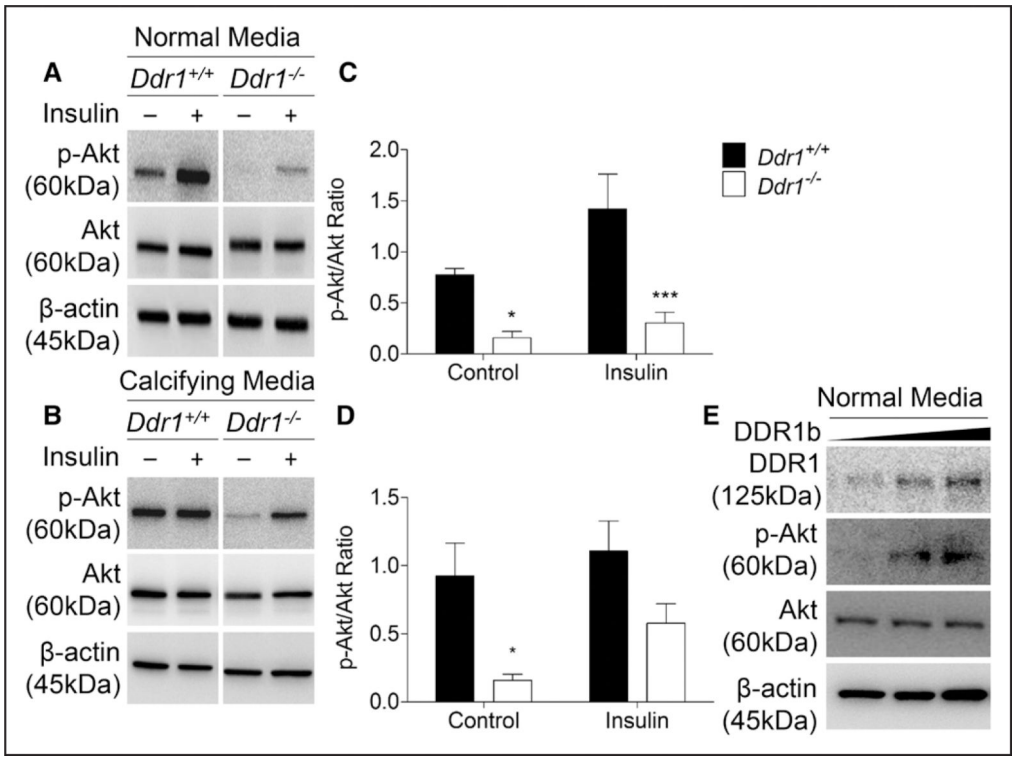

Figure 3.

Discoidin domain receptor 1 (DDR1) modulates p-Akt levels in vascular smooth muscle cells (VSMCs). *Ddr1*$^{+/+}$ and *Ddr1*$^{-/-}$ VSMCs were treated with control or insulin (10 nmol/L) and probed for p-Akt after 2 d in normal (**A**) or calcifying media (**B**). In normal media, *Ddr1*$^{-/-}$ VSMCs had significantly lower p-Akt levels with or without insulin treatment (**C**). In calcifying media, p-Akt levels were significantly lower in *Ddr1*$^{-/-}$ VSMCs compared with *Ddr1*$^{+/+}$ VSMCs at baseline but not when treated with insulin (**D**). Full-length DDR1b was transfected into *Ddr1*$^{-/-}$ VSMCs, resulting in rescue of p-Akt activation (**E**). **C** and **D**, Two-way ANOVA with Bonferroni post hoc test (**P*<0.05, ****P*<0.001 comparing *Ddr1*$^{+/+}$ to *Ddr1*$^{-/-}$ VSMCs).

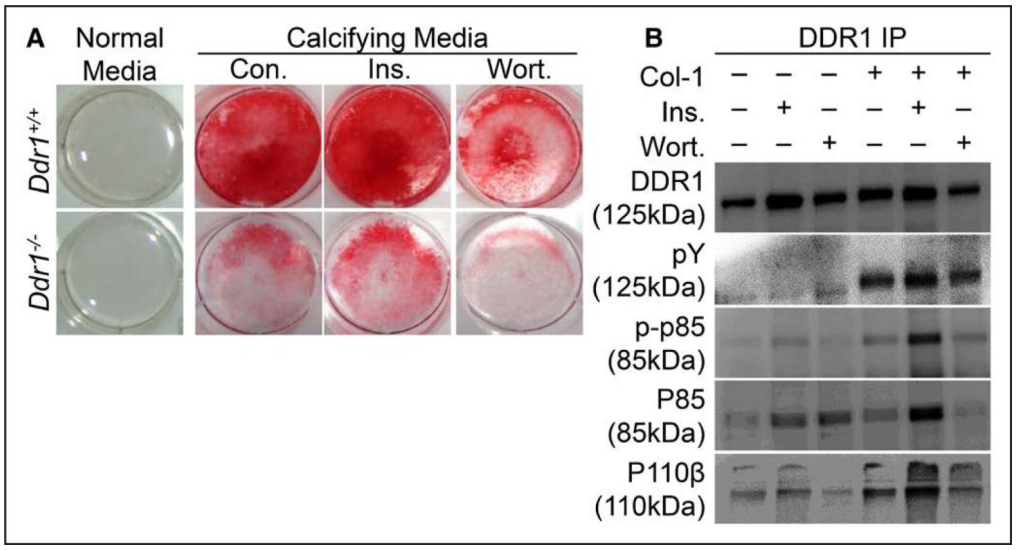

Figure 4.

Discoidin domain receptor 1 (DDR1) mediates vascular smooth muscle cell (VSMC) calcification through the phosphoinositide 3-kinase (PI3K)/Akt signaling axis. *Ddr1*$^{+/+}$ and *Ddr1*$^{-/-}$ VSMCs were cultured in calcifying media for 12 d and treated daily with dimethyl sulfoxide (Con.), insulin (Ins.), or wortmannin (Wort.) (**A**). Insulin stimulated VSMC calcification while wortmannin attenuated calcification. DDR1 immunoprecipitation was performed on cell lysates from *Ddr1*$^{+/+}$ VSMCs treated with insulin, wortmannin, or type-I collagen (Col-1) (**B**). Treatment with Col-1 led to increased DDR1 activation (pY), and Col-1 or insulin treatment resulted in increased association of DDR1 with PI3K subunits (p110β and p85). Wortmannin attenuated this interaction.

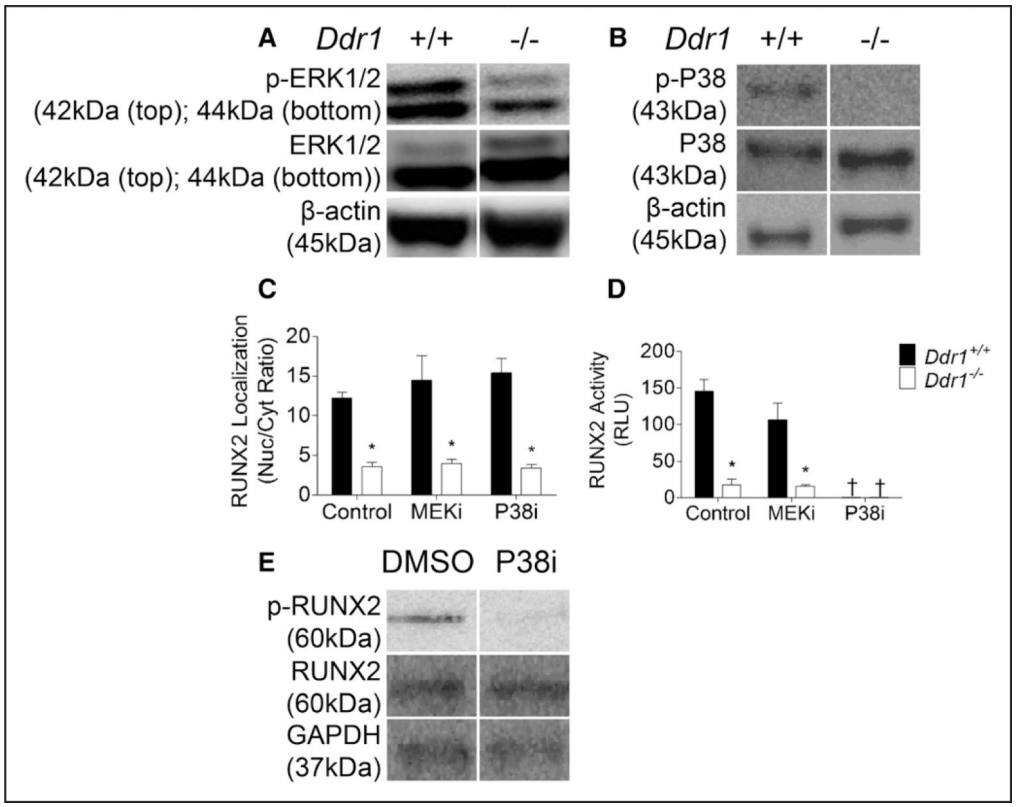

Figure 5.

Discoidin domain receptor 1 (DDR1) deletion affects ERK1/2 (extracellular signal-related kinase 1/2) and P38 mitogen activated protein kinase (P38) activity; P38 is required for RUNX2 (runt-related transcription factor 2) phosphorylation and activation. *Ddr1*$^{+/+}$ and *Ddr1*$^{-/-}$ VSMCs were cultured in normal media for 2 d and probed for ERK1/2 and P38 (**A** and **B**, respectively). RUNX2 nuclear localization was not affected by MEK (MAPK/ERK kinase) or P38 inhibition (**C**). RUNX2 activity (**D**) and phosphorylation (**E**) were reduced after P38 inhibition. **C** and **D**, Two-way ANOVA with Bonferroni post hoc test (*P<0.05 comparing *Ddr1*$^{+/+}$ to *Ddr1*$^{-/-}$ VSMCs; †P<0.05 comparing inhibitor to dimethyl sulfoxide [DMSO] control). RLU indicates relative luminescence units.

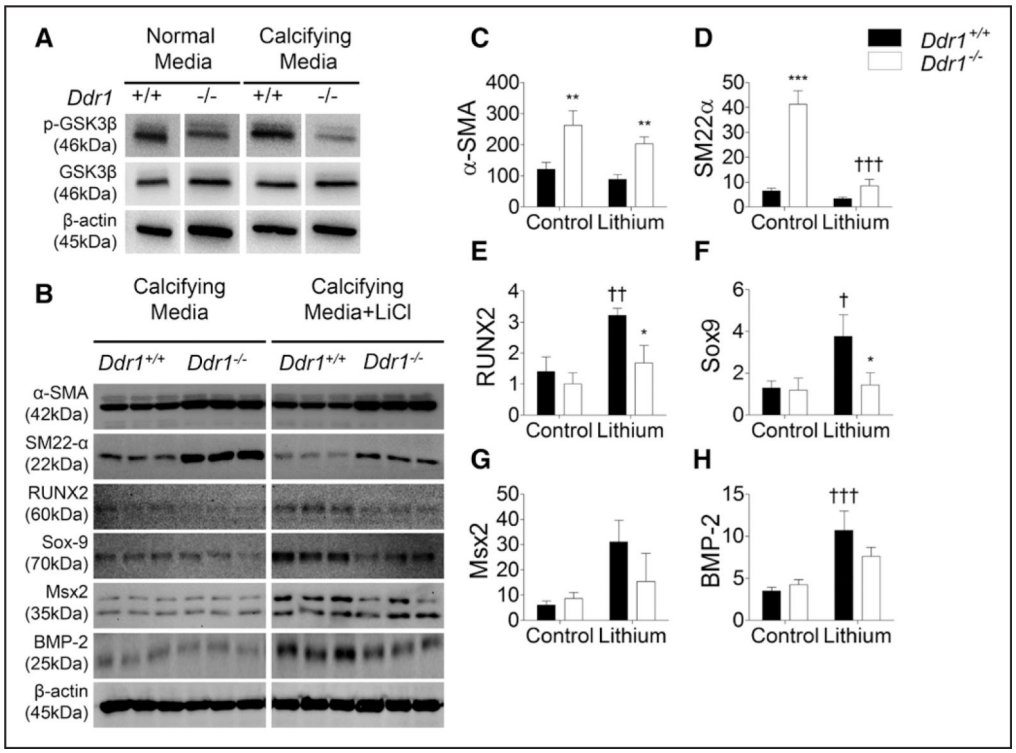

Figure 6.

Glycogen synthase kinase (GSK) 3β inhibition results in an increase in osteochondrogenic marker expression in *Ddr1*$^{+/+}$ but not *Ddr1*$^{-/-}$ vascular smooth muscle cells (VSMCs). VSMCs were cultured in normal or calcifying media for 12 d and probed for phospho-GSK3β (p-GSK3β), revealing lower expression of p-GSK3β (inactive form) in *Ddr1*$^{-/-}$ VSMCs (**A**). VSMCs were subsequently cultured in calcifying media in the presence or absence of lithium chloride (LiCl; 20 mmol/L), and expression of osteogenic and smooth muscle markers was assessed by immunoblot (**B**). Smooth muscle marker expression was significantly higher in *Ddr1*$^{-/-}$ VSMCs (**C** and **D**). Osteochondrogenic markers RUNX2 (runt-related transcription factor 2; **E**), Sox-9 (sex-determining region-Y box-9; **F**), Msx2 (Msh homeobox 2; **G**), and BMP-2 (bone morphogenetic protein-2; **H**) were upregulated with LiCl treatment in *Ddr1*$^{+/+}$ but not *Ddr1*$^{-/-}$ cells. **C**–**H**, Two-way ANOVA with Bonferroni post hoc test (*P<0.05, **P<0.01, ***P<0.001) comparing *Ddr1*$^{+/+}$ to *Ddr1*$^{-/-}$ VSMCs; †P<0.05, ††P<0.01, †††P<0.001 comparing LiCl to control.

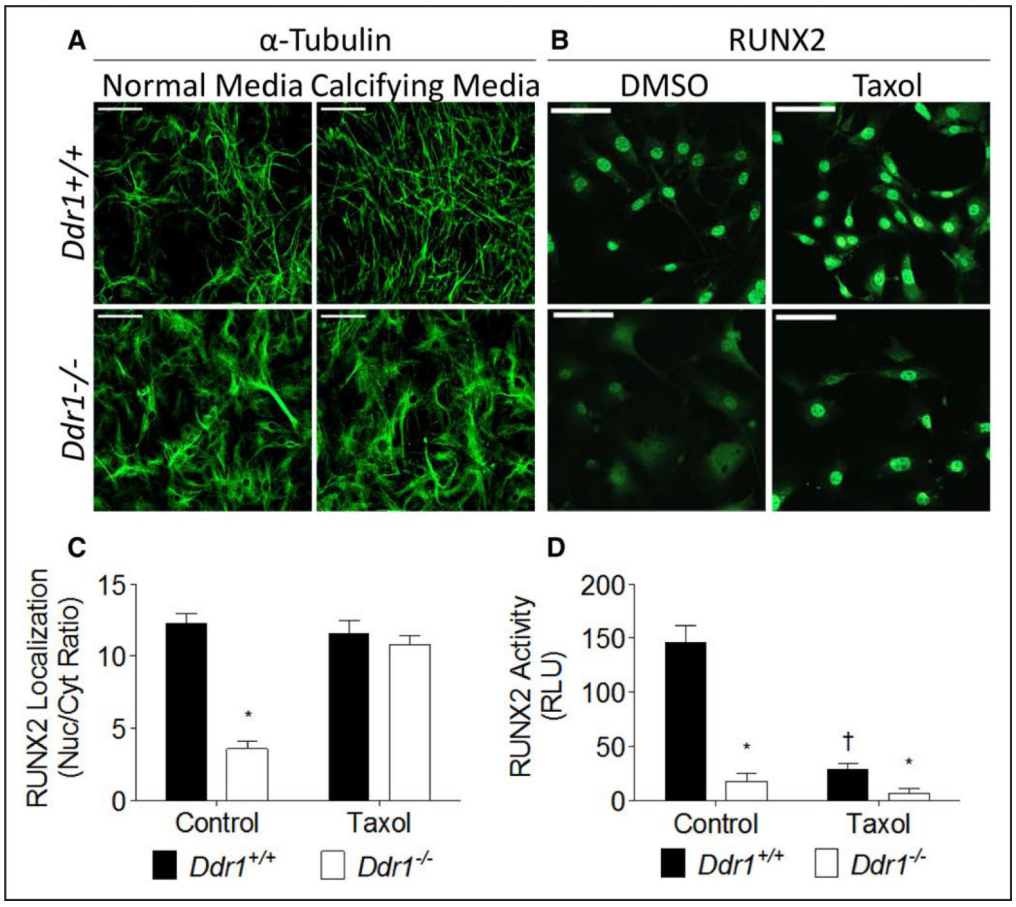

Figure 7.

Microtubules are disrupted in *Ddr1*$^{-/-}$ vascular smooth muscle cells (VSMCs), and stabilization of microtubules with taxol rescues RUNX2 (runtrelated transcription factor 2) nuclear localization but not activity. *Ddr1*$^{+/+}$ and *Ddr1*$^{-/-}$ VSMCs cultured in normal and calcifying media were immunostained for α-tubulin (**A**). VSMCs treated with taxol were immunostained for RUNX2 (**B**). RUNX2 nuclear localization was rescued by treatment of *Ddr1*$^{-/-}$ cells with taxol (**C**), whereas RUNX2 activity was impaired in both *Ddr1*$^{-/-}$ and *Ddr1*$^{+/+}$ VSMCs treated with taxol (**D**). **A**, Scale bars, 200 μm; (**B**), scale bars, 20 μm. **C** and **D**, Two-way ANOVA with Bonferroni post hoc test (*P<0.05 comparing *Ddr1*$^{+/+}$ to *Ddr1*$^{-/-}$ VSMCs; †P<0.05 comparing taxol to control). RLU indicates relative luminescence units.